Evaluation method for time-dependent corrosion depth of uncoated weathering steel using thickness of corrosion product layer

Shigenobu Kainuma[1a], Yuya Yamamoto[2b], Jin-Hee Ahn[3c], Young-Soo Jeong[*4]

[1]*Department of Civil Engineering, Kyushu University, 744, Motooka, Fukuoka 8190395, Japan*
[2]*Planning Department, Japan Expressway Holding and Debt Repayment Agency, 1-1-2, Takashima, Yokohama 2200011, Japan*
[3]*Department of Civil Engineering, Gyeongnam National University of Science and Technology,
33 Dongjin-ro, Jinju, Gyeongnam 52725, Republic of Korea*
[4]*Seismic Simulation Test Center, Pusan National University, 49 Busandaehak-ro, Yansan, Gyeongnam 50612, Republic of Korea*

Abstract.   The corrosion environments in a steel structure are significantly different depending on the individual parts of the members. To ensure the safety of weathering steel structures, it is important to evaluate the time-dependent corrosion behavior. Thus, the progress and effect of corrosion damage on weathering steel members should be evaluated; however, the predicted corrosion depth, which is affected by the corrosion environment, has not been sufficiently considered until now. In this study, the time-dependent thicknesses of the corrosion product layer were examined to quantifiably investigate and determine the corrosion depth of the corroded surface according to the exposure periods and corrosion environments. Thus, their atmospheric exposure tests were carried out for 4 years under different corrosion environments. The relationship between the thickness of the corrosion product layers and mean corrosion depth was examined based on the corrosion environment. Thus, the micro corrosion environments on the skyward and groundward surfaces of the specimens were monitored using atmospheric corrosion monitor sensors. In addition, the evaluated mean corrosion depth was calculated based on the thickness of the corrosion product layer in an atmospheric corrosion environment, and was verified through a comparison with the measured mean corrosion depth.

Keywords: corrosion depth; corrosion product layer; weathering steel; atmospheric exposure test; electro-magnetic coating thickness tester

1. Introduction

Weathering steel has been adopted for steel bridges because of the decrease in repainting costs. The design of weathering steel bridges excludes the application of a protective coating, and thus the steel is permitted to rust at an uncontrolled rate. However, when in contact with airborne salt, anti-freezing agents, moisture and fugitive dust, the surfaces of the members do not form a protective rust layer in steel structural members. The corrosivity of the structural member and the time-dependent corrosion behavior are important factors in ensuring that weathering steel bridges can be used safely while remaining economical.

Previous studies regarding the corrosion damage of weathering steel have typically been conducted to verify the corrosion durability and the corrosion environment by measuring the corrosion loss of anti-corrosion techniques, including atmospheric exposure tests based on the assumption of a conventional power-law function (Kawabata *et al.* 2004, Chen *et al.* 2005, Kamimura *et al.*

2006). In a predication model for the long-term corrosion loss response of weathering steel, the durable state concept and a series of sequential phase models have been applied (Kihira *et al.* 2005a, b, Melchers 2008). However, these tests cannot evaluate the thickness of the corrosion product layer and corrosion environments, which emphasizes the importance of the maintenance of steel structures to increase their service life. Based on these problems, corrosion monitoring has been applied using several different types of sensors (Nishikata *et al.* 2005, 2014, Wall *et al.* 2005, Schindelholz *et al.* 2013). On the other hand, atmospheric corrosion monitor (ACM) type corrosion sensors have been used to evaluate corrosion environments (Motoda *et al.* 1994, 1995, Kainuma *et al.* 2011). However, monitoring systems used in corrosion environments of steel structures require expensive sensors and loggers and the durability of the sensors is significantly decreased in corrosion environments characterized by airborne sea salt. In some cases, replacement sensors are required approximately every month. The corrosivity of structural members on a long span bridge cannot be evaluated using these methods because of the requirement for multiple monitoring locations and the application of ACM sensors. Thus, the requirements of a useful evaluation method for corrosion damage during a pre-investigation phase using ACM sensors for structural environment monitoring and a corrosion factor analysis have been emphasized. Severe corrosion damage has occurred on the members of steel

*Corresponding author, Research Professor
  E-mail: ysjung@pusan.ac.kr
[a]Associate Professor
[b]M.Sc.
[c]Assistant Professor

(a) Kyushu University (KU)

(b) Fukuoka Kita-kyushu Highway (FM)
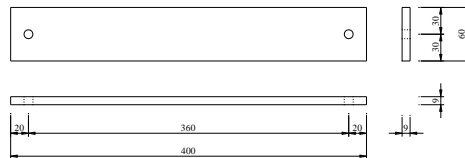

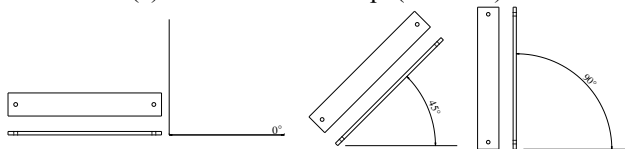(c) University of the Ryukyus (UR)

(d) Okinawa Highway (NK)

Fig. 1 Atmospheric exposure test field

(a) Dimension and shape(unit:mm)

(b) Test set-up of atmospheric exposure test specimen

Fig. 2 Dimension of atmospheric exposure test specimen

Table 1 Chemical composition of test specimen (mass %)

C	Si	Mn	P	S	Cu	Ni	Cr
0.13	0.25	1.03	0.013	0.006	0.31	0.10	0.49

Table 2 Average temperature, relative humidity, precipitation and airborne sea salt in each exposure field

Test field	Temperature (K)	Relative humidity (%)	Precipitation (mm)	Airborne sea salt (mg·dm^{-2}/day)
KU	289	75	1,721	0.41
FM	291	66	1,758	0.57
UR	296	74	2,103	0.29
NK	296	74	2,293	0.68

bridge exposed to a lengthy wet-period, usually owing to rain, dew, mist, as well as by deposited and accumulated airborne sea salt and anti-freezing agents. However, it is difficult to comprehensively evaluate the corrosivity of a member from an individual evaluation of each corrosion factor because of the possibility of interference and the time-dependent characteristics, which can develop a method for comprehensively evaluating the corrosivity depending on the galvanic corrosion current of an ACM sensor. The condition of the protective rust layer has been evaluated based on the thickness of the corrosion product layer

formed on the members of weathering steel bridges (Miura *et al*. 2006, Kainuma *et al*. 2012, Kihira *et al*. 2013). However, it was not evaluated for the time-dependent corrosion behavior based on the thickness of the corrosion product layer.

In this study, the time-dependent thicknesses of the corrosion product layer were examined to quantifiably investigate and determine the corrosion depth of a corroded surface according to the exposure periods and corrosion environments. Thus, atmospheric exposure tests were carried out for 4 years, and four test fields were chosen

because the corrosion characteristics differed. The effect of the atmosphere on the thickness of the corrosion product layers was examined. In addition, the temperature, humidity and airborne sea salt (using a dry gauze method) were measured. The micro-corrosion environments on the skyward and groundward surfaces of the specimens were monitored using ACM sensors. In addition, a method for evaluating the mean corrosion depth using the thickness of the corrosion product layer was suggested.

2. Atmospheric exposure test

2.1 Atmospheric exposure test conditions and specimens

To examine the corrosivity of steel members under atmospheric environments, atmospheric exposure tests on weathering steel plates were conducted for 1, 2, 3 and 4year periods. In the case of a corrosion problem, the amount of airborne salt, moisture, and sand puddle, along with their interaction and time-dependent effects are significant factors. Thus, four test fields were selected to determine the time-dependent corrosion factors under atmospheric corrosion environments as shown in Fig. 1. The test conditions of each test field are described below.

1) The KU test field is on the Ito Campus of Kyushu University (lat. 33°35′ N, long. 130°12′ E), which is 2.9 and 5.3 km from the eastern and western coastlines of northern Kyushu, respectively. This test field is characterized by high rainfall, but not high quantities of airborne sea salt.

2) The FM test field is under the Fukuoka Kita-kyushu Highway, 50 m from the northern coastline near Momochi beach (lat. 33°35′ N, long. 130°21′ E). This test field is characterized by airborne sea salt but not rainfall.

3) The UR test field is on the Senbaru Campus of the University of the Ryukyus (lat. 26°15′ N, long. 127°46′ E) 2.3 and 4.4 km from the eastern and western coastlines of Okinawa Island, respectively. This test field is characterized by high rainfall and airborne sea salt.

4) The NK test field is under the Okinawa Highway, 30 m from the west coastline of Kyoda, Okinawa Island (lat. 26°32′ N, long. 127°57′ E). This test field is characterized by high quantities of airborne sea salt but not rainfall.

The test specimens used for atmospheric exposure were uncoated weathering steel plates (JIS G 3114 (2008)) with a length, width, and thickness of 400, 60, and 9 mm, respectively, as shown in Fig. 2(a). Table 1 shows the chemical compositions of the test specimens. To consider the various corrosion conditions based on their details and installation, the steel structural members were installed at angles of 0°, 45°, and 90° to the horizontal direction, as shown in Fig. 2(b). For the test specimens at an angle of 90°, the north-facing surface was defined as skyward in the UR and KU test fields. The seaside surface was also defined as skyward in the test specimens in the FM test field. In addition, to examine the effects of rainfall and airborne sea salt in twenty different corrosion environments, ACM Fe/Ag galvanic couple type sensors (output of 0.1 nA to 10 mA, and resolution of 0.1 nA (0.1 nA to 10 μA) to 1 μA (1 μA to 10 mA)) were installed on the skyward and

(a) Dimension and shape(unit:mm)
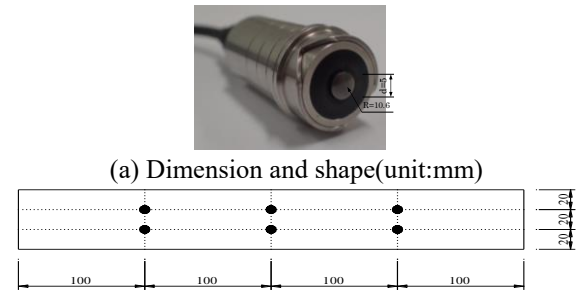
(b) Measurement point of corrosion product layer of specimen

Fig. 3 Dimension and shape of electromagnetic coating thickness meter(unit:mm)

groundward surfaces of the specimens (Motoda *et al*. 1955). These sensors were replaced monthly as a result of their decreasing output sensitivity due to sensor deterioration. Table 2 shows the measured corrosion environment data in terms of temperature(T), relative humidity(RH), precipitation(P) and airborne sea salt(w) (measured using a dry gauze method according to JIS Z 2382 (1998)). The average temperature during the 4-year test period in the UR and NK test fields was 5°C higher than that of the KU and FM fields. The relative humidity was within the same range (74-75%) for the UR, NK, and KU fields, which is greater than the 66% recorded for the FM field. The precipitation was measured as 2,100 mm in the UR and NK test fields, but approximately 20% lower in the KU and FM fields. The airborne sea salt had the highest value (0.68 mg·dm^{-2}/day) in the NK field, followed by 0.57 mg·dm^{-2}/day in the FM field, and 0.41 mg·dm^{-2}/day in the KU field, whereas that of the UR field was only 0.29 mg·dm^{-2}/day.

2.2 Analysis method of rust layers

To evaluate the corrosion level according to the fractions of three constituent elements (Fe, O, and Si) in the rust, the rust layers formed on each aged corrosion specimen were analyzed using an X-ray diffraction technique (XRD). Different oxyhydroxides of α-FeOOH, β-FeOOH, γ-FeOOH and Fe_3O_4 formed in the rust layer (Yamashita *et al*. 1994, Wang *et al*. 2013). The measurements were carried out using a RINT-1500 diffractometer with a Cu target under the condition of 40kV to 200 mA. The ZnO was mixed at the same ratio of 30% of the corrosion products. Spectra were collected for a 2θ value between 10.0° and 16.2°, 19.0° and 23.5°, and 29.0° and 32.5°. Images of the cross-sections were taken using a scanning electron microscope (SEM), and an energy-dispersive electron-probe microanalysis (EMPA), with a 15 kV acceleration voltage, was used for the qualitative analysis of the light elements such as Fe, O, and Si, on the specimen surfaces.

2.3 Measurement method of the thickness of the corrosion product layer and calculation method of mean corrosion depth

The measured thicknesses of the corrosion product

Table 3 Composition of corrosion products on skyward surface of specimen (wt%)

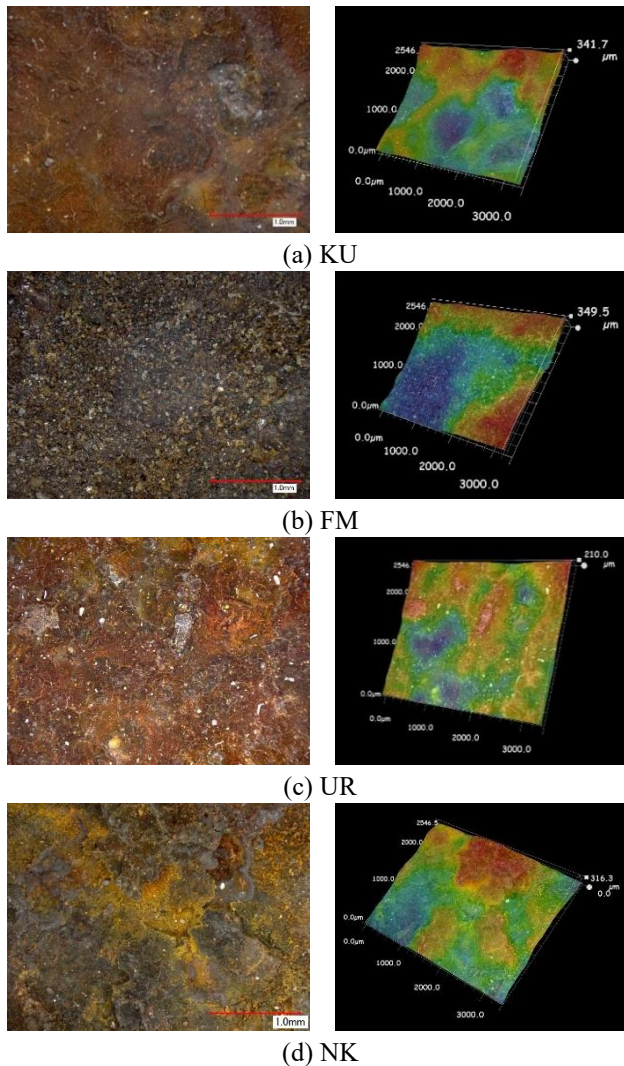| Test field	Installation angle (°)	Exposed period (year)	α	β	γ	Fe₃O₄	Non-crystalline
KU	45	1	12.5	0.4	37.7	0.3	47.9
FM	45	1	7.6	54.4	9.5	0	9.1
UR	45	3	14.2	1.6	35.4	1.9	46.9
NK	0	1	10.9	15.5	20.2	0	53.4

(a) KU

(b) FM

(c) UR

(d) NK

Fig. 4 Corroded surface of specimens depending on skyward surface for installation of 0° after exposure for 4 years
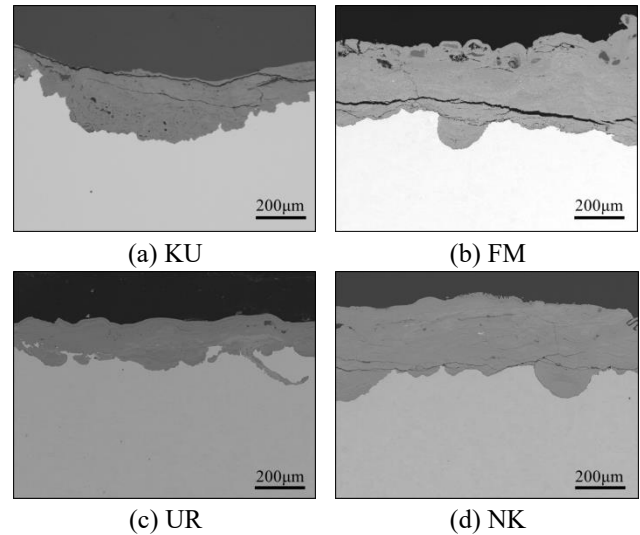

(a) KU   (b) FM

(c) UR   (d) NK

Fig. 5 SEM images for cross-sectional corrosion product layer at skyward surface of specimens after exposure for 2 years

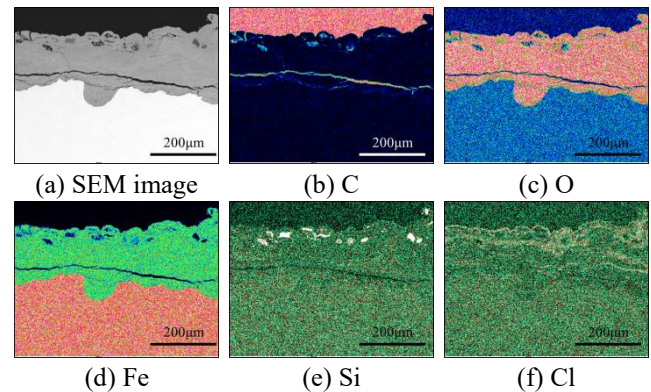(a) SEM image   (b) C   (c) O

(d) Fe   (e) Si   (f) Cl

Fig. 6 EPMA elemental maps of Fe, O and Si for cross-sectional corrosion product layer at 45° skyward surface of specimens after exposure for 2 years

layers on the test specimens after the atmospheric exposure tests were conducted using an SM-1000 (Sanko Electronic Laboratory Co., Ltd) electro-magnetic coating thickness tester, as shown in Fig. 3(a). When iron is moved away from a steel core coil, changes in self-inductance between the steel core and magnetic metallic substrate occur and can be read using an ammeter. The tester specifications include a measurement accuracy of ±1 μm, and resolution of 1 μm (0 to 999 μm), and 10 μm (1 to 8 mm) with a one-point contact (probe tip diameter of 5 mm, and curvature of 10.6 mm). Thus, the effect on the measurement accuracy for the thickness of the corrosion product layer when using the electro-magnetic coating thickness tester was evaluated, and compared with the microscope results. As the results indicate, the thickness of the corrosion product layer was affected by the Fe components in the corrosion products, however, the results of the electro-magnetic coating thickness tester were approximately less than 10% of those of the microscope results regardless of the exposure field and corrosion environment. To measure the thicknesses of the corrosion product layers, the probe tip was changed to a diameter and curvature of 5 and 3.6 mm, respectively, which showed a similar tendency (Kainuma *et al.* 2012).

To take into consideration the variation in the measured value, the thickness of the corrosion product layer was measured by taking eleven measurements at six points, as shown Fig. 3(b). The measurement of weight loss is typically used to calculate the change in thickness of a corroded steel plate. The corrosion products were removed using ammonium citrate at 60°C, and a nylon brush (Kainuma *et al.* 2012). A laser focus measuring system (spot diameter of 30 μm, and resolution of 0.05 μm) was

used to measure the corrosion depth on the corroded surface after removal of the rust for each aged corrosion specimen. The mean corrosion depth was calculated as a combination of weight loss and the configuration of the corrosion surface.

3. Atmospheric exposure test results

3.1 Composition of corrosion products and characteristics of surface and cross section

3.1.1 Composition of corrosion products

The quantitative analysis results of the corrosion products on the test specimen are summarized in Table 3. β-FeOOH is a typical component of a rust layer developed in marine atmospheric environments (Ma *et al*. 2009). The specimens in the NK and FM fields were shown to not be directly influenced by the rain-wash effect, with results of 15.5% and 54.4%, respectively. Thus, these areas can be considered as comparatively high corrosive environments for steel structures. However, specimens in the UR and KU fields showed results of approximately 1.6% and 0.4%, respectively, because of the rain-wash effect (Kihira *et al*. 2013). It was reported that β-FeOOH can contain up to 6% chloride and can form during an early corrosion stage in chloride containing electrolytes through the hydrolysis of $FeCl_3$ or oxidation of $FeCl_2$ in the presence of iron. Moreover, the corrosion products of weathering steel in atmospheric exposure environments were evaluated to be at a relatively stable stage in the UR and KU fields, because the rust layer was comprised of approximately 12% α-FeOOH. The main constituent of the rust layers formed on weathering steels was altered from lepidocrocite through an amorphous substance into goethite, the goethite layer of which may be the final form of the protective rust layer (Misawa *et al*. 1974, Misawa 2001). In addition, the amount of non-crystalline products, which include FeOOH and Fe_3O_4, was approximately 40%, regardless of the exposure field, which is characteristic of the corrosion products in an atmospheric environment.

3.1.1 Characteristics of corroded surface

To identify rust on a corrosion surface as a result of atmospheric exposure tests, the appearance of each test specimen was confirmed through microscope images, as shown in Fig. 4. Thus, skyward surfaces images of the 4-year atmospheric test specimens were compared for cases with an installation angle to the horizontal direction of 0°, because all surface images were shown to be similar regardless of their facing direction. The skyward surfaces that were exposed to rainfall are shown to be relatively smooth from a rain-wash effect through a high level of precipitation (P), as shown in Figs. 4(a) and 4(c).

In contrast, for the specimens in the FM (Fig. 4(b)) and NK (Fig. 4(d)) fields, the corrosion product layers are shown to have relatively porous surfaces owing to a lack of rain-wash effect by rainfall on the deposited airborne sea salt particles. For the 4-year exposed specimen in the NK field, partial detachment of the corrosion product layer was found, because the rain-wash effect on the deposited

(a) KU	(b) FM
(c) UR	(d) NK

0-0.03
0.03-0.06
0.06-0.09
0.09-0.12
0.12-0.15
0.15-0.18
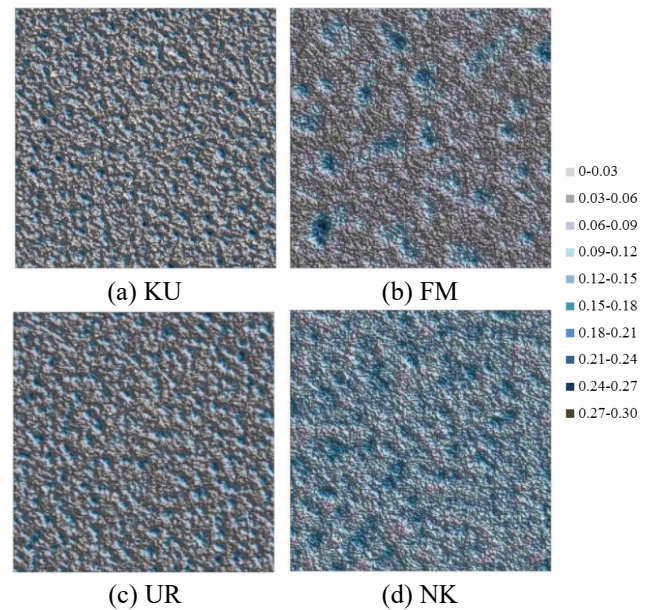0.18-0.21
0.21-0.24
0.24-0.27
0.27-0.30

Fig. 7 Corrosion depth of corroded surface for skyward at 0° after removal of corrosion product after 4 years on exposure field(40×40 mm)

airborne sea salt by rain was insufficient.

3.1.3 Characteristics of cross section on corroded specimen

Fig. 5 shows an SEM image of the cross-section of the corrosion product layer in each exposure field. The KU, FM, and UR fields are represented by the 45° skyward specimen, and the NK field is represented by the 0° skyward specimen. In Fig. 5, they are also shown to have similar surface characteristics. Fig. 6 shows the EPMA results of the corrosion product for the 45° skyward specimen after 2 years in the FM field. Si appeared near the surface of the corrosion product layer, and sand and existing rust were shown to have combined and progressed. In addition, the presence of Cl was confirmed near the surface, and was affected by the airborne sea salt.

In this study, a laser focus measuring system (spot diameter of 30 μm and spatial resolution of 0.05 μm) was used to measure the corrosion surface characteristics, such as the mean, maximum, and minimum corrosion depths after the removal of rust on each corrosion specimen, as shown Fig. 7. The surface images of the corroded steel plates for various exposure periods were evaluated to obtain corrosion characteristic image data of the surfaces of the corroded steel plates. For each corrosion specimen, corrosion surface images were acquired for specimens of all installation angles. Although the appearance of surface roughness seems to vary slightly depending on the exposure field, the corrosion morphology can be classified as uniform corrosion. The surfaces of the specimens in the KU and UR fields were affected by rain-wash, and small-scale corrosion pitting can be seen compared to specimens in the FM and NK fields. In particular, the corrosion pitting and surface roughness of the corroded surfaces of specimens in the FM and NK fields are larger than those of the KU and UR fields. Thus, the corrosion figuration of the skyward surface
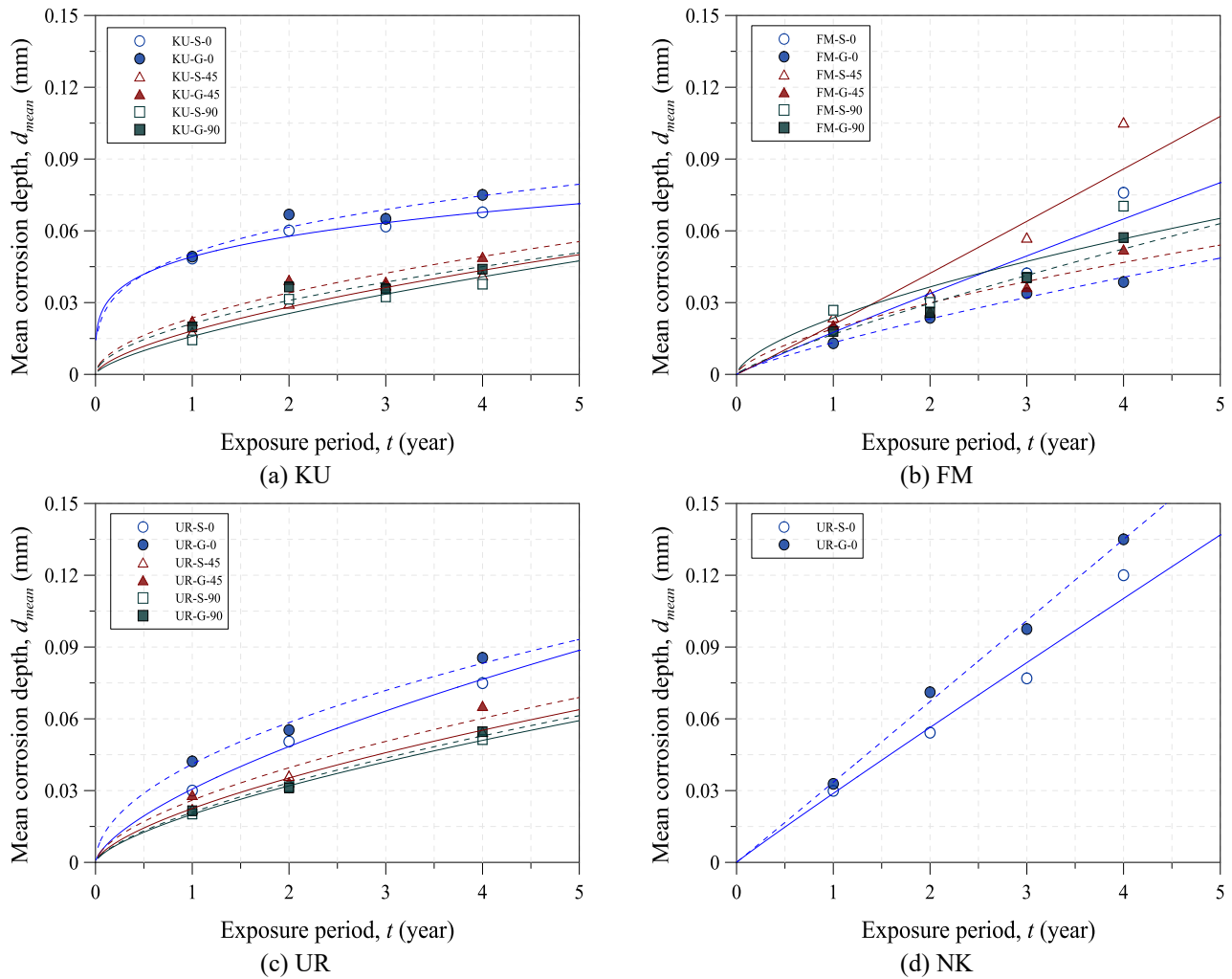
(a) KU

(b) FM

(c) UR

(d) NK

Fig. 8 Mean corrosion depth of tested surface as a function of exposure period

on the specimen in the FM field is different than that of the groundward surface, and is influenced by accumulated salt without a rain-wash effect.

3.2 Corrosion loss of corroded surface for each exposure

Fig. 8 shows the change in the mean corrosion depth of the corrosion specimens for each exposure period. The corrosion loss of the weathering steel plate in the atmospheric environment was shapely changed at an early corrosion stage, but gradually decreased with an increase in the exposure period. The corrosion is thought to accelerate owing to the presence of chloride and pollutants, and as the pitting develops through further corrosion, their corrosion rates were shown to decrease as a result of the protective action of the existing rust. The relationships of mean corrosion depth and exposure period vary appreciably depending on the surface direction (skyward or groundward), as well as on the installation angle in the exposure field. These relationships vary significantly from one exposure field to another. The effect of the installation angle on the magnitude of the mean corrosion depth appears to be larger than that between the skyward surface and the groundward surface. For the skyward surfaces of specimens

with installation angles of 0° and 45° in the FM and NK fields, the mean corrosion depth is shown to have a linear relationship with the exposure period because their corrosion product layers do not protect against additional corrosion. This is due to pores present in the corrosion product layers as a result of the deposition and accumulation of airborne sea salt. In the following equation, factor b for these test specimens was designated as 1.0.

$$d_{mean} = a \cdot t^b \qquad (1)$$

Here, b=-12.3·a+0.916 for a situation with no adhesion of sea salt particles and

b=1 for a situation with deposition of airborne sea salt, where, d_{mean} is the mean corrosion depth (mm), t is the exposure period (year), and a and b are constants.

Table 4 shows the relationship between mean corrosion depth and exposure period, as well as its relation coefficient values with regard to Eq. (1). Table 4 shows the values of the coefficients a, and b and the corresponding correlation factor R, which is no less than 0.9 for any test piece, suggesting a high significance of the acquired data. The values of factor b vary depending on the installation angle, as well as on their facing directions. This is caused by
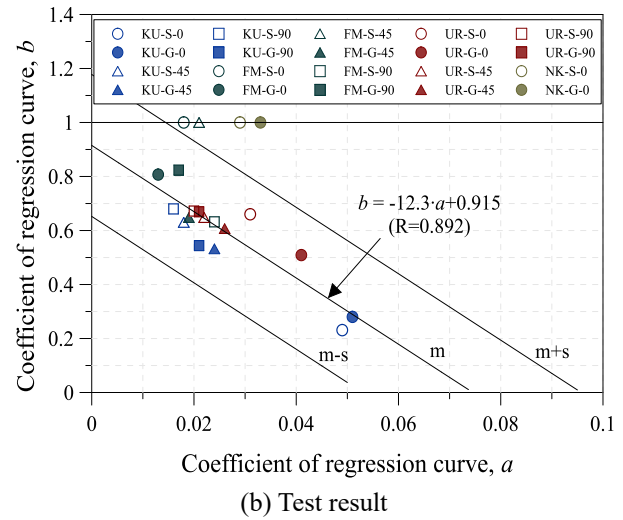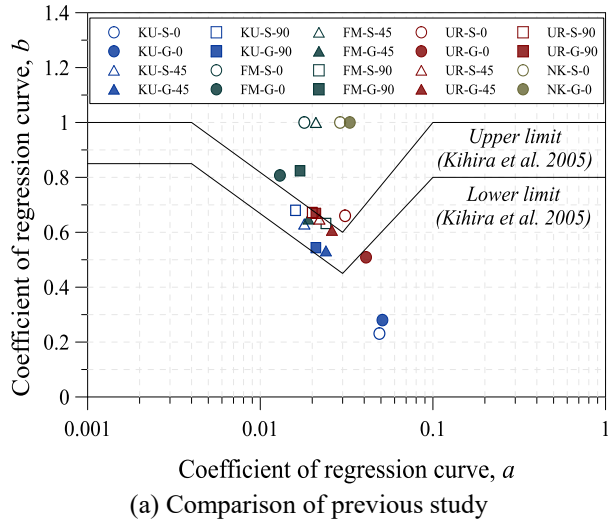
(a) Comparison of previous study

(b) Test result

Fig. 9 Relationship between coefficients *a* and *b* of regression curves

Table 4 Mean corrosion depths-exposed period relation

Test field	Installation angle		Coefficient		Correlation coefficient
			a	b	
KU	0°	Skyward	0.049	0.231	0.979
		Groundward	0.051	0.280	0.940
	45°	Skyward	0.018	0.630	0.993
		Groundward	0.024	0.532	0.951
	90°	Skyward	0.016	0.680	0.944
		Groundward	0.021	0.544	0.945
FM	0°	Skyward	0.018	0.934 (1)	0.976
		Groundward	0.013	0.807	0.996
	45°	Skyward	0.022	0.962 (1)	0.934
		Groundward	0.019	0.648	0.962
	90°	Skyward	0.024	0.632	0.882
		Groundward	0.017	0.824	0.979
UR	0°	Skyward	0.031	0.66	0.997
		Groundward	0.041	0.509	0.991
	45°	Skyward	0.023	0.646	0.999
		Groundward	0.026	0.607	0.947
	90°	Skyward	0.020	0.673	1.000
		Groundward	0.021	0.669	0.993
NK	0°	Skyward	0.036	1.20 (1)	0.996
		Groundward	0.044	1.00 (1)	1.00

study, the relationship between correlations *a* and *b* was evaluated by considering the corrosion environments, as shown in Fig. 9(b). The correlation between *a* and *b* is roughly inversely proportional, except for the test specimens in the FM field with installation angles of 0° and 45° in the skyward direction, and in the NK field with an installation angle of 0° in both the skyward and groundward direction. The correlation coefficient *a* tends to increase with increasing precipitation (*P*), implying a trend in promoting the initial corrosion by rainwater. In an environment with high precipitation (*P*), the washing-away effect of the formed corrosion product seems to be promoted, leading to the formation of a dense protective corrosion product layer and diminished values of *b*. On the other hand, in an environment with low precipitation (*P*), such as FM, the value remained low owing to a small initial mean corrosion depth. Nevertheless, the corrosion product layer in the FM field became porous, diminishing its protectiveness, and leading to an increase in *b*. As pointed out earlier, the corrosion product layer, formed in an environment with a high deposition rate of airborne sea salt particles will lose its corrosion protectiveness. In summary, the values of factor *b* are represented.

4. Evaluation of time-dependent corrosion depth based on thickness of corrosion product layer

4.1 Thickness of corrosion product layer of corroded surface depending on exposure period

The thicknesses of the corrosion product layers on the corroded surfaces of the atmospheric exposure specimens were examined to evaluate the changes in the steel surfaces owing to corrosion damage, using an electro-magnetic coating thickness tester. Fig. 10 shows the thicknesses of the corrosion product layers of the test specimens. The variation in the thicknesses of the corrosion product layers on the FM and NK specimens is larger than that of the KU and UR specimens, and the rain-wash effect was shown to have no direct influence in this regard. The variation shows
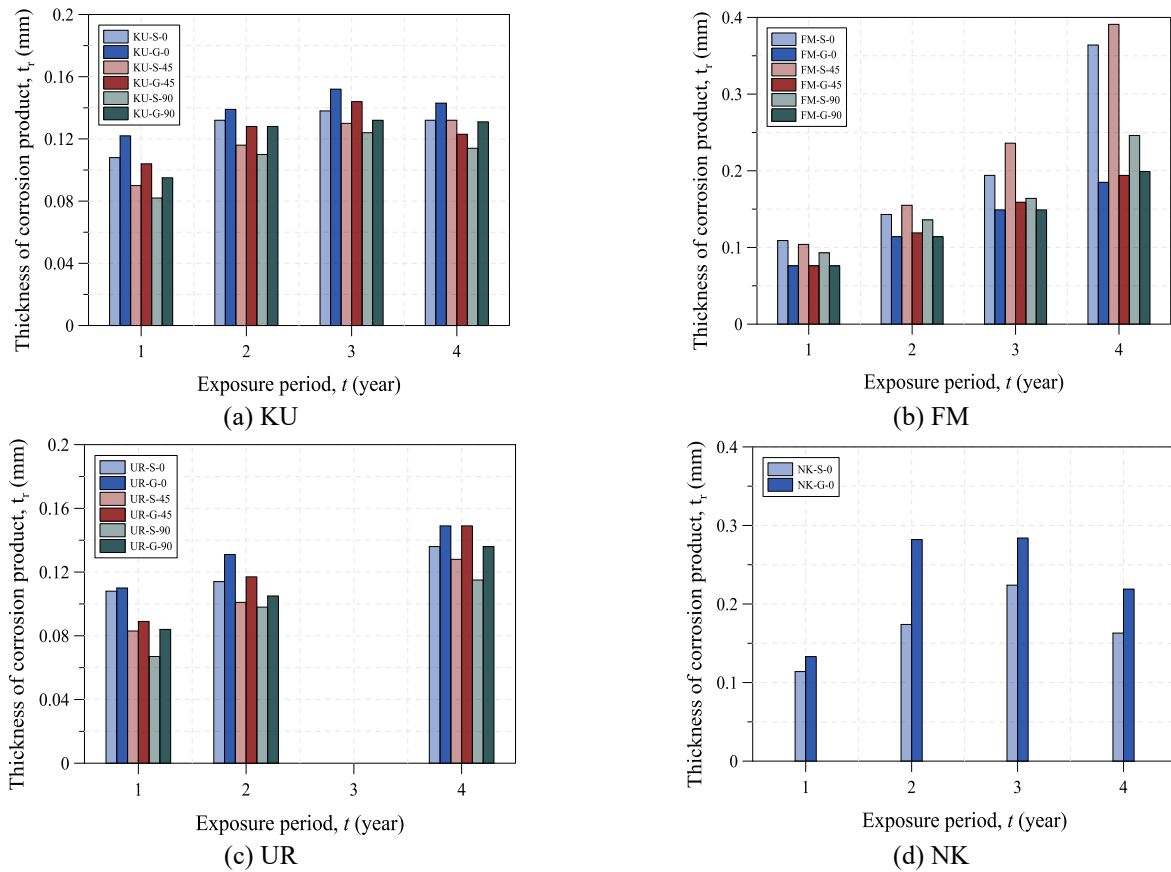
precipitation (*P*) and the washing-away effect on the deposited airborne sea salt, which are affected by their installation conditions.

Fig. 9(a) shows the relationship between correlations *a* and *b*, it was simply divided to direction at vertical and horizontal at 41 bridge in Japan, but the corrosion environments were different in same structural member as exposure period, rain-wash effect and airborne sea salt etc. (Kihira *et al*. 2005a, b). Although there is possibility that the value of *b* may be a function of exposure period. In this

(a) KU

(b) FM

(c) UR

(d) NK

Fig. 10 Variations in measuring thickness of corrosion product layer
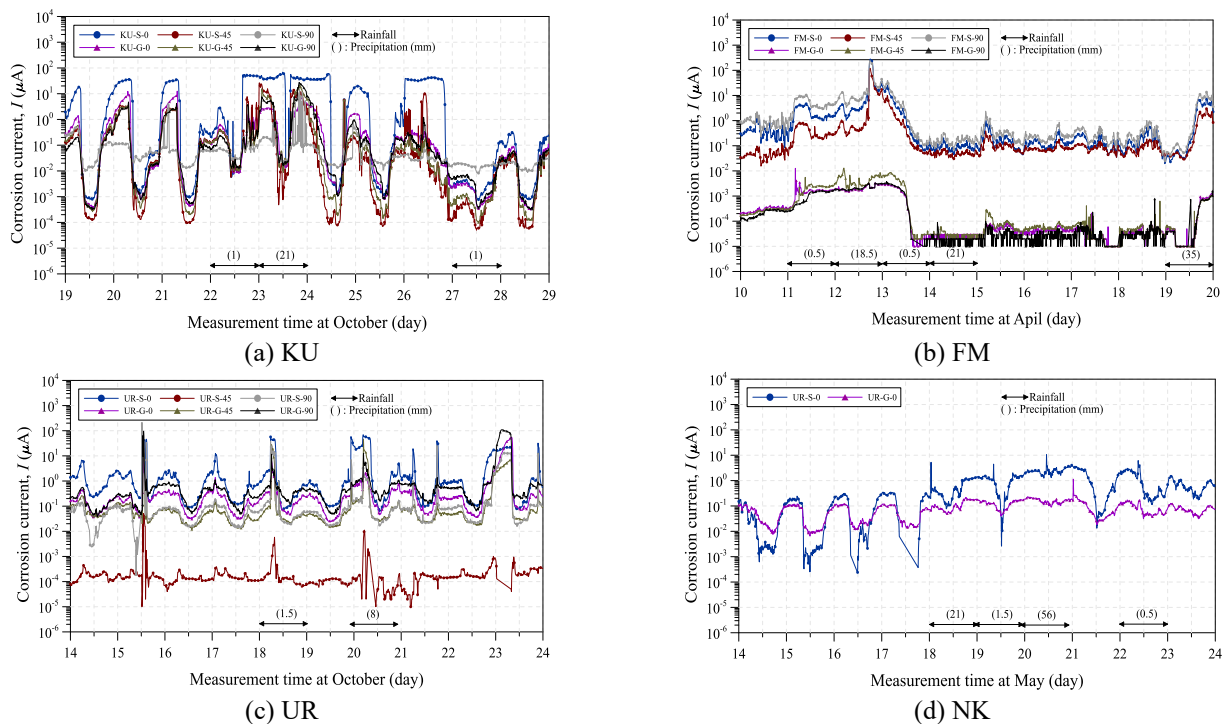

(a) KU

(b) FM

(c) UR

(d) NK

Fig. 11 Variation of ACM sensor current on exposure field

the same tendency regardless of the exposure field and installation angle. The mean thicknesses of the corrosion product layers of the corrosion specimens according to the exposure periods. The mean thicknesses of the corrosion product layers of the FM specimens are shown to increase according to the exposure period (year) in corrosive atmospheric environments. The corrosion environment of NK is similar to that of FM, however, depending on the

exposure period, a decreasing tendency was shown, as a result of porous surfaces from a lack of a rain-wash effect. The mean thicknesses of the UR and KU specimens for an exposure period of three years is either constant, or decreases as a result of the rain-wash effect.

When a thin water film forms on a steel surface, the ACM sensor interprets it as rainfall or dew, and a galvanic current passes between the substrate (Fe) and the conductive paste (Ag). It has been reported that this galvanic current shows a good correlation with the corrosion rate of actual metals, such as steel and zinc. Thus, by measuring the ACM sensor output, it is possible to evaluate the corrosion environments quantitatively. To verify the measured current using an ACM sensor in an atmospheric corrosion environment, it was compared with Meteorological Agency data, including on a day withobserved rain, as shown Fig. 11 (Kainuma *et al.* 2014). The ACM sensor output for rainfall was greater than 1 μA (rainfall threshold), and that for dew was greater than 0.1 μA (dew threshold) (Shinohara *et al.* 2005). In the case of the KU and UR specimens, the current was shown to be greater than 1 μA on a rainy day. Currents of over 1 μA occurring on other days seem to be due to condensation in the morning. The currents on the skyward surfaces of the KU and UR specimens increased in the following order of installation angle, 90°, 45° and 0°, and were shown to be affected by rainfall. The currents on the skyward surface of the NK specimens were larger than those of the groundward surfaces, which is likely due to the difference in the amount of salt that adhered to the surfaces. Thus, the FM sky and groundward specimens were different because of the sandy beach on the northern side, approximately 10 m away. It seems that sand is easily included in the salt and moisture on the surface.

$$d_{mean} = \alpha \cdot t_{r,mean} \qquad (2)$$

Here, α=0.242(0.064≤ $t_{r,mean}$≤0.392 for an environment without a rain-wash effect

α=0.287(0.065≤ $t_{r,mean}$≤0.158 for an environment with a rain-wash effect, and

α=0.416(0.096≤ $t_{r,mean}$≤0.152 for stagnant environment with rainfall

where, d_{mean} is the mean corrosion depth (mm), $t_{r,mean}$ is the thickness of corrosion product layer (mm), and α a constants.

Fig. 12 shows the relationship between the mean corrosion depth and the thickness of the corrosion product layer, as well as the related coefficient values with regard to Eq. (2). In the case of test fields KU and UR, the thickness of the corrosion product increased slightly with increase in the mean corrosion depth. The values of the FM and NK field specimens gradually increased with the mean corrosion depth. This is thought to be accelerated by chloride, without a rain-wash effect. Thus, the thickness of the corrosion product layer is shown to change according to the installation angle. It is a different tendency because of the corrosion environment according to the installation angle and exposure field. Consequently, to examine the relationship of mean corrosion depth-thickness of the corrosion product layer and corrosion environment, the
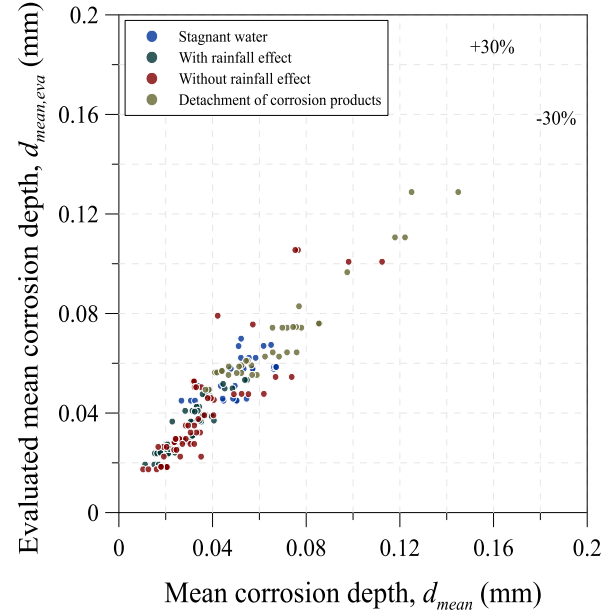

Fig. 13 Validation of mean corrosion depth calculated by using Eq. (5)

environments were classified as stagnant water, and with and without a rain-wash effect, as shown in Fig. 12(b). For a cases of the corrosion environment under stagnant water conditions and with a rain-wash effect, the thickness of the corrosion product layer was less than 0.15 mm, but whereas without a rain-wash effect, it was increased with an increase in the mean corrosion depth.

4.2 Comparison between measured and evaluated mean corrosion depths

The corrosion damage in steel members varies according to atmospheric environment parameters, such as temperature, humidity, rainfall and wind direction. In this study, the corrosion depths of the corroded steel members are used to express the thicknesses of the corrosion product layers formed on the surfaces of the specimens. It is assumed that the environment remains constant.

$$d_{mean,1year} = a \qquad (3)$$

where, $d_{mean,1year}$ is the mean corrosion depth for an exposure period of 1year(mm), and a is a constant.

The mean corrosion depth after 1 year can be calculated using Eq. (1). Therefore, it is possible to estimate the relationship of constant (a) between the thickness of the corrosion product and the mean corrosion depth for an exposure period of 1 year, as shown in Fig. 7. The constant (b) can be calculated using the mean corrosion depth and the exposure period. From the calculated constants (a and b) of the corroded specimens under each atmospheric condition, a time-dependent mean corrosion depth was evaluated using the thickness of the corrosion product layers.

$$d_{mean,1year} = d_{mean,1year} \cdot t^b \qquad (4)$$

Here, $b=-12.3 \cdot d_{mean,1year}+0.916$ for a situation with no adhesion of sea salt particles, and

$b=1$ for a situation with the deposition of airborne sea salt

where, d_{mean} is the mean corrosion depth (mm), $d_{mean,1year}$ is the mean corrosion depth for an exposure period of 1 year, t is the exposure period (year), and b is a constant.

To verify the evaluated mean corrosion depth using the thickness of the corrosion product layer in an atmospheric corrosion environment, the evaluated mean corrosion depths were compared with the measured mean corrosion depths for each corrosion environment, as shown in Fig. 13. The mean corrosion depth of real corroded steel was shown to be similar to the evaluated mean corrosion depth by within 30%. Therefore, the change in thickness of a structural steel member of weathering steel can be estimated based on time-dependent corroded surface values under a real corrosion environment. And it can be useful for examining behaviors and safety margin of corroded steel structures using providing data by evaluation results.

5. Conclusions

In this study, the mean corrosion depths of weathering steel were evaluated according to the corrosion environment. An atmospheric exposure tests were carried out over a period of 4 years at four exposure fields to examine the effects of individual corrosion environments. The corrosion depths were analyzed using a typical evaluation method and the thickness of the corrosion product layer. The mean corrosion depth and thickness of the corrosion product layer of each tested specimen were compared according to the corrosion period. As the results indicate, the relationships between the mean corrosion depth and the exposure time varied appreciably depending on whether the exposed surfaces are skyward or groundward, as well as on the installation angle of the exposure field. The effect of the installation angle on the magnitude of the mean corrosion depth appears to be larger than that between the skyward surface and the groundward surface. For the high quantities of airborne sea salt at the tested field, the mean corrosion depth is shown to have a linear relationship with the exposure period. Therefore, the variation in thickness of the corrosion product layer shows the same tendency regardless of the exposure field and installation angle. In addition, the mean corrosion depth was calculated based on the measured thickness of the corrosion product layer. The evaluated mean corrosion depth was shown to be similar to the real corroded surface of specimen by within 30%. Future research, evaluating the effect of the different corrosion environments on the mean corrosion depth, and a continuous evaluation of individual parts in corroded steel structures, will be conducted.

Acknowledgments

References

Chen, Y.Y., Tzeng, H.J., Wei, L.I., Wang, L.H., Oung, J.C. and Shih, H.C. (2005), "Corrosion resistance and mechanical properties of low-alloy steels under atmospheric conditions", *Corros. Sci.*, **47**(4), 1001-1021.

JIS G 3114 (2008), *Hot-Rolled Atmospheric Corrosion Resisting Steels for Welded Structure*, Japan Industrial Standards, Japan.

JIS Z 2382 (1998), *Determination of Pollution for Evaluation of Corrosivity of Atmospheres*, Japan Industrial Standards, Japan.

Kainuma, S., Yamamoto, Y., Itoh, Y. and Oshikawa, W. (2011), "Prediction method for mean corrosion depth of uncoated carbon steel plate subjected to rainfall effect using Fe/Ag galvanic couple ACM-type corrosion sensor", *Corros. Eng.*, **60**(11), 498-503.

Kainuma, S., Yamamoto, Y., Itoh, Y., Hayashi, H. and Oshikawa, W. (2012), "Evaluation method for corrosion depth of uncoated carbon steel and its time-dependence using thickness of corrosion product layer", *Corros. Eng.*, **61**(12), 483-494.

Kainuma, S., Yamamoto, Y., Itoh, Y., Hayashi, H. and Oshikawa, W. (2014), "Practical method for estimating time-dependent corrosion depth of uncoated carbon steel plate under atmospheric environment using Fe/Ag galvanic couple ACM-type corrosion sensor", *Corros. Eng.*, **63**(2), 50-67.

Kamimura, T., Hara, S., Miyuki, H., Yamahita, M. and Uchida, H. (2006), "Composition and protective ability of rust layer formed on weathering steel exposed to various environments", *Corros. Sci.*, **48**(9), 2799-2812.

Kawabata, F., Matsui, K., Obinata, T., Komori, T., Takemura, M. and Kubo, T. (2004), *Steel Plates for Bridge Use and Their Application Technologies*, JFE Technical Report No. 2, JFE Steel.

Kihira, H., Senuma, T., Tanaka, M., Nishioka, K., Fujii, Y. and Sakata, Y. (2005), "A corrosion prediction method for weathering steels", *Corros. Sci.*, **47**(10), 2377-2390.

Kihira, H., Shiotani, K., Miyuki, H., Nakayama, T., Takemura, M. and Watanabe, Y. (2013), "Systematic interpretation of rust evaluation methods for weathering steels", *J. Civil Eng.*, **745/1-65**, 77-87.

Kihira, H., Tanabe, K., Kusunoki, T., Takezawa, H., Tasunami, H., Tanaka, M., Matsuoka, K. and Harada, Y. (2005), "Mathematical modeling to predict long-term corrosion loss to occur on weathering steel", *J. Civil Eng.*, **780/1-70**, 71-86.

Ma, Y.T., Li, Y. and Wang, F.H. (2009), "Weatherability of 09CuPCrNi steel in a tropical marine environment", *Corros. Sci.*, **51**(8), 1725-1732.

Melchers, R.E. (2008), "A new interpretation of the corrosion loss processes for weathering steels in marine atmospheres", *Corros. Sci.*, **50**(12), 3446-3454.

Misawa, T. (2001), "Research progress on corrosion science of iron and steels", *Corros. Eng.*, **50**(12), 538-545.

Misawa, T., Asami, K., Hashimoto, K. and Shimodaira, S. (1974), "Mechanism of atmospheric rusting and protective amorphous rust on low-alloy steel", *Corros. Sci.*, **14**(4), 279-289.

Motoda, S., Suzuki, Y., Shinohara, T., Kojima, Y., Tsujikawa, S., Oshikawa, W., Itomura, S., Fukushima, T. and Izumo, S. (1994). "ACM (atmospheric corrosion monitor) type corrosion sensor to evaluate corrosivity of marine atmosphere", *Corros. Eng.*, **43**(10), 550-556.

Motoda, S., Suzuki, Y., Shinohara, T., Tsujikawa, S., Oshikawa, W., Itomura, S., Fukushima, T. and Izumo, S. (1995), "Corrosive factors of a marine atmosphere analyzed by ACM sensor for 1 year", *Corros. Eng.*, **44**(4), 253-265.

Nishikata, A., Suzuki, F. and Tsuru, T. (2005), "Corrosion monitoring of nickel-containing steels in marine atmospheric environment", *Corros. Sci.*, **47**(10), 2578-2588.

Nishikata, A., Zhu, Q. and Tada, E. (2014), "Long-term monitoring of atmospheric corrosion at weathering steel bridges by an electrochemical impedance method", *Corros. Sci.*, **87**, 80-88.

Schindelholz, E., Kelly, R.G., Cole, I.S., Ganther, W.D. and Muster, T.H. (2013), "Comparability and accuracy of time of wetness sensing methods relevant for atmospheric corrosion", *Corros. Sci.*, **67**, 233-241.

Shinohara, T., Motoda, S. and Kshikawa, W. (2005), "Evaluation of corrosivity of atmosphere by ACM type corrosion sensor", *Corros. Eng.*, **54**(8), 375-382.

Wall, F.D., Martines, M.A., Missert, N.A., Copeland, R.G. and Kilgo, A.C. (2005), "Characterizing corrosion behavior under atmospheric conditions using electrochemical techniques", *Corros. Sci.*, **47**(1), 17-32.

Wang, Z.F., Liu, J.R., Wu, L.X., Han, R.D. and Sun, Y.Q. (2013), "Study of the corrosion behavior of weathering steels in atmospheric environments", *Corros. Sci.*, **67**, 1-10.

Yamashita, M., Miyuki, H., Matsuda, Y., Nagano, H. and Misawa, T. (1994), "The long-term growth of the protective rust layer formed on weathering steel by atmospheric corrosion during a quarter of a century", *Corros. Sci.*, **36**(2), 283-299.

CC